# Numerical simulation of columns with un-bonded reinforcing bars for crack control

G. Chen[†]

*Queensland University of Technology, QLD 4001, Australia*

H. Fukuyama[‡], M. Teshigawara[‡†], H. Etoh[‡‡], K. Kusunoki[‡‡†], and H. Suwada[‡‡‡]

*Building Research Institute, 1 Tachihara, Tsukuba, Ibaraki 305-0802, Japan*

**Abstract.** Following previous work carried out in Building Research Institute in Japan, finite element analyses of conceptual column designs are performed in this paper. The effectiveness of the numerical model is evaluated by experimental tests and parametric studies are conducted to determine influential factors in conceptual column designs. First, three different column designs are analysed: bonded, un-bonded, and un-bonded with additional reinforcing bars. The load-displacement curves and cracking patterns in concrete are obtained and compared with experimental ones. The comparisons indicate that the finite element model is able to reflect the experimental results closely. Both numerical and experimental results show that, the introduction of un-bonded zones in a column end can reduce cracking strains, accordingly reduce the stiffness and strength as well; the addition of extra reinforcement in the un-bonded zones can offset the losses of the stiffness and strength. To decide the proper length of the un-bonded zones and the sufficient amount of the additional reinforcing bars, parametric studies are carried out on their influences. It has been found that the stiffness of un-bonded designs slightly decreases with increasing the length of the un-bonded zones and increases with the size of the additional reinforcing bars.

**Keywords:** column; concrete; reinforcement; cracking; bond-slip; finite element method; non-linear analysis.

## 1. Introduction

Reinforced concrete (RC) members are structurally designed such that they have excellent deformation capacity, which may absorb large energy due to earthquakes. However, severe cracking and crushing of concrete usually occur after yielding of steel. Cracking in yielding zone reduces the compressive capacity of the concrete, which leads to the loss of strength and the deformation

† Ph.D., JSPS Research Fellow, Corresponding author, E-mail: g3.chen@qut.edu.au
‡ Chief Researcher, E-mail: fukuyama@kenken.go.jp
‡† Professor, E-mail: teshi@corot.nuac.nagoya-u.ac.jp
‡‡ Visiting Researcher, E-mail: h_eto@kenken.go.jp
‡‡† Senior Researcher, E-mail: kusunoki@kenken.go.jp
‡‡‡ Senior Researcher, E-mail: suwada-h92h9@nilim.go.jp.

capacity of the RC members. Besides, serious cracking in concrete structures brings psychological distresses to occupants and incurs expensive repair costs. Better control of concrete cracking can maintain the compressive capacity, durability, and shear resistance of concrete structures; it also protects structural appearance and reduces repair costs.

Current design practice for concrete structures in seismic regions is intended to result in inelastic response at the selected plastic hinge regions during strong ground shaking; all other regions of structure are then made adequately strong to ensure that the inelastic deformations occur only at the selected plastic hinge regions and that failures due to shear, bond splitting, and loss of reinforcement anchorage are avoided. Column footings and beam-column joints are usually at the hinge regions and undergo severe cracking under strong ground shaking. Joint behaviors have been the subject of intense experimental and theoretical studies for some time (Bonacci and Pantazopoulou 1993, Hakuto *et al.* 2000, Mazzoni and Moehle 2001, Megget 1973, Tajima *et al.* 2000). Column failure mechanism has also been well investigated (Hallgren and Bjerke 2002, Harumi Yashiro *et al.* 1990, Maekawa and An 2000, Mau 1990, Saadeghvaziri 1997). However there are very few studies in the literature on controlling concrete cracking in column ends. Recently Hiraishi *et al.* (2004) and Teshigawara *et al.* (2004) proposed a conceptual design, in which the bond between reinforcing steel and concrete was removed in column ends by introducing an un-bonded zone. Their experimental results demonstrated that the cracking patterns in the column ends are significantly improved. The crack numbers reduce and the cracks become shorter in the new conceptual designs, which could substantially diminish the repair work to recover the original structural performance after earthquakes. The idea of introducing an un-bonded zone was first used by Hamada *et al.* (1978) and Goto *et al.* (1987) and followed by Ichinose (1991), Matsuoka *et al.* (1999), and Kashiwazaki and Noguchi (1994) to investigate the bond influence in beam-column joints. Pandey and Mutsuyoshi (2005) experimentally investigated the seismic performance of RC piers reinforced with different bond conditions, varying from perfectly bonded to completely un-bonded; their results revealed that the failure mode at the ultimate state could change from shear to flexure by reducing the bond strength of the longitudinal bars.

Fig. 1 schematically shows the cracking patterns of the column ends with and without an un-bonded zone. Under a lateral loading, the column end is at the critical section. The first crack occurs along the column bottom line. Without introducing an un-bonded zone, cracking area develops upwards along the main re-bar. With the introduction of an un-bonded zone, no stress is transferred from the main reinforcing bar to the surrounding concrete in this zone. After the first
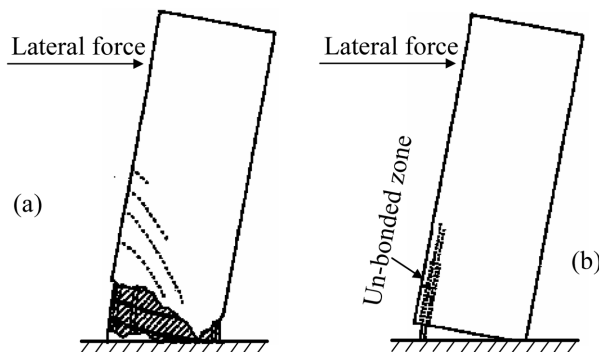


Fig. 1 Cracking damage in column footings. (a) conventional design, (b) design with un-bonded zone
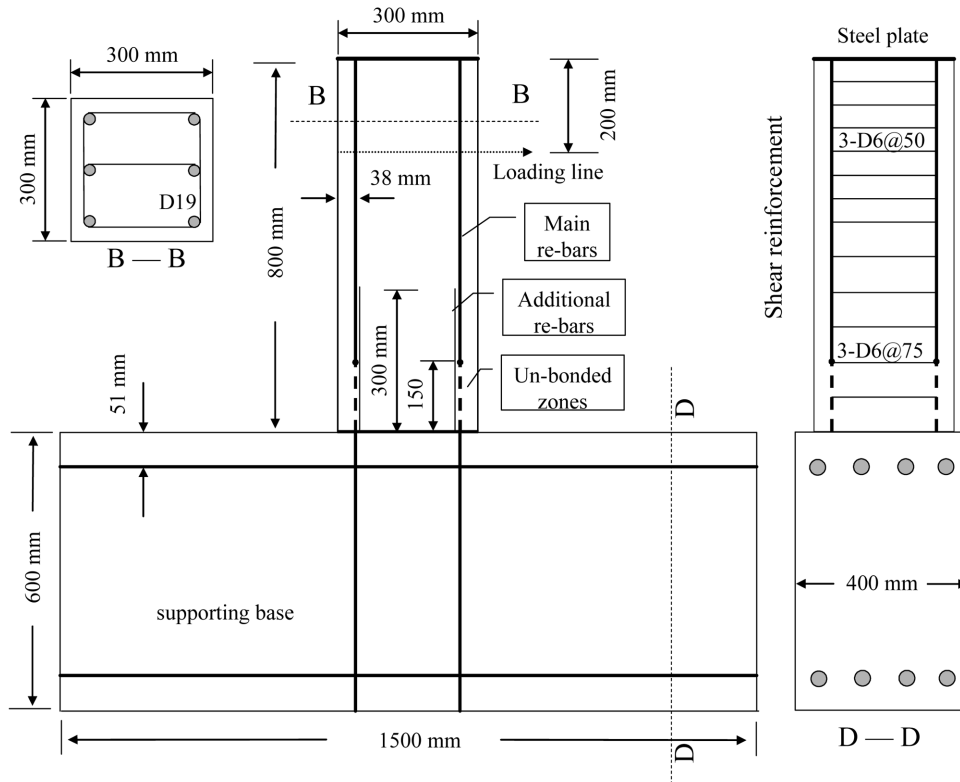
Fig. 2 Column with supporting base

crack forms at the column bottom, the stress in the concrete surrounding the un-bonded zone is released. It is expected that the introduction of the un-bonded zone can diminish cracking and shear strength degradation in the un-bonded zone.

Previous researches (Hiraishi *et al.* 2004, Teshigawara *et al.* 2004) were based on the experimental methodology that requires a large number of test specimens, takes long time, and hardly covers all the influencing factors. On the other hand, if its effectiveness is verified by the experimental tests, the finite element model would be economical and easily-implemented, and be able to provide the most detailed information of the influencing parameters and serve as a design and evaluation tool.

This paper aims to develop a non-linear finite element model to study the behaviors of column ends. Cracking in concrete is modeled by a "total strain rotating model" and the bond-slip by a non-linear interface relation (DIANA 2002b). Following Hiraishi *et al.* (2004) and Teshigawara *et al.* (2004), un-bonded zones are introduced in column ends. As shown in Fig. 3, three different column designs are analysed: bonded, un-bonded, and un-bonded with additional reinforcing bars. In the un-bonded cases, the main reinforcing bars in the column end are separated from the surrounding concrete. For the third case, the additional re-bars are added around the un-bonded zones and completely embedded in concrete. By comparing the results, the mechanism of the conceptual column designs will be studied and assessed. It is expected that introducing un-bonded zones (in the column end) is able to control structural damage like tensile cracking along the column surface. At
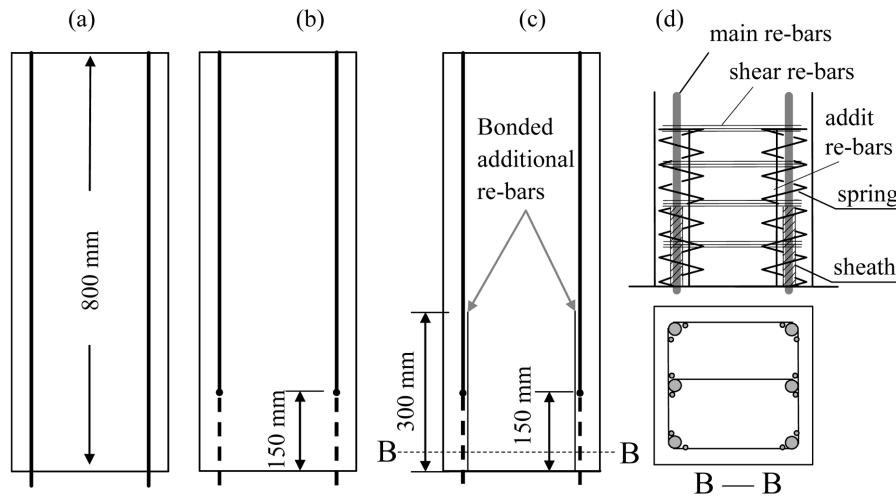
Fig. 3 Column design. (a) Bonded, (b) Un-bonded (D24-A00), (c) Un-bonded with additional re-bars (D24-A06), (d) Arrangement of additional re-bars

the same time, introducing an un-bonded zone will reduce the global flexural and shear resistance of the column, it is anticipated that introducing additional re-bars will offset these losses. The proposed FE model will be employed to study the influences of the un-bonded zones and the additional re-bars.

## 2. Conceptual designs of column ends

The geometry of the considered column is shown in Fig. 2. The column has dimensions of 300 × 300 mm in cross section and 800 mm in height. The column is connected to and supported by a strong base which has the dimensions of 400 × 600 × 1500 mm. The column is reinforced by 6 deformed reinforcing bars with a diameter of 19 mm. The reinforcement arrangement is shown in Fig. 2. The shear reinforcing bars in the column are arranged in the centre-to-centre distance of 75 mm at the lower part and 50 mm at the upper part (see D-D section), with each line representing three shear reinforcing bars with a diameter of 6 mm. On the top of the column a steel plate is affixed, to which all the main reinforcing bars are welded.

This paper considers three designs for the column: bonded, un-bonded, and un-bonded with additional reinforcing bars (Fig. 3). For the bonded design, the (main) reinforcing steel has a complete bond with the surrounding concrete; for the un-bonded designs, in the column end, the reinforcing steel is fully separated from the surrounding concrete via a sheath [see Fig. 3(d)], shown by the dashed parts in Figs. 3(b),(c). The length of the un-bonded zones is 150 mm. For the third design, the reinforcing steel in the column end is completely separated from the surrounding concrete and additional reinforcing bars are added around the main reinforcing bars [Fig. 3(d)]. The additional re-bars (two around each main bar), which are fully bonded with surrounding concrete, go from the column bottom line up to 300 mm as shown in Figs. 3(c), (d). The additional reinforcing bars have a diameter of 6 mm. In the third design, a spring is spiralling around the main re-bars and the additional re-bars, which prevents the buckling of the main re-bars. As no buckling

is observed in the experimental tests, the spring is not considered in the numerical analysis.

The supporting base is reinforced by 8 deformed reinforcing bars with a diameter of 22 mm. As the main concern is column cracking, the supporting base is designed much stiffer and stronger than the column and the influences of its shear reinforcing bars are not considered here. The design details are seen in Teshigawara *et al.* (2004).

In the following context, different lengths of un-bonded zones and different sizes of additional re-bars will be considered. There are totally 4 different lengths of un-bonded zones: 75 mm, 150 mm, 225 mm, and 300 mm (i.e., $\frac{1}{4}D$, $\frac{2}{4}D$, $\frac{3}{4}D$, and $\frac{4}{4}D$, where $D$ is the column width) and 3 sizes of additional re-bars (6 mm, 12 mm, and 18 mm in diameter). To distinguish them, a symbol system is employed. Except the bonded design, all others are named like D*4-A**, where D*4 means that the length of the un-bonded zone is $\frac{*}{4}D$ and A** represents the size of the additional re-bars, with the wild mark "*" representing a digit. For instance, D14-A00 symbolizes a design with a $\frac{1}{4}D$ un-bonded zone and no additional re-bars, and D24-A06 a design with a $\frac{2}{4}D$ un-bonded zone and additional re-bars with a diameter of 6 mm. By using this naming system, the three designs experimentally tested are represented by "Bonded", "D24-A00", and "D24-A06". The length of the additional re-bars is 150 mm plus the length of the corresponding un-bonded zones.

## 3. Experimental overview

Fig. 4 shows the loading setup, in which the hatched areas represent moment distributions. The secondary moment is ignored since the deformation angle is small. The specimens are loaded in two directions. A constant axial load of 425 KN is applied on the column top during the entire loading process and a cyclic lateral load applied to the column at the loading point via an actuator. The lateral loading is controlled by the deformation angle as shown in Fig. 5. The loading is applied until the specimens are unable to sustain the constant axial load. Displacement transducers are used
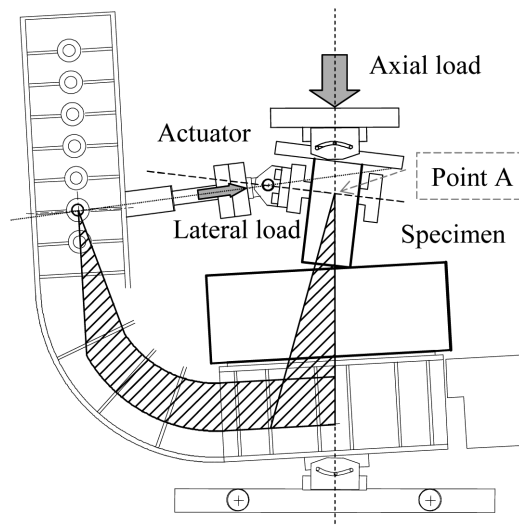


Fig. 4 Experimental setup
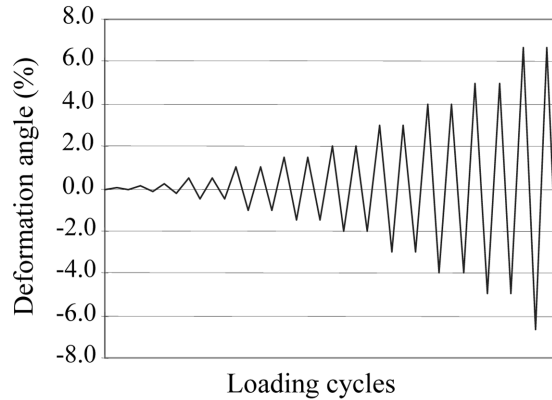
Fig. 5 Loading process
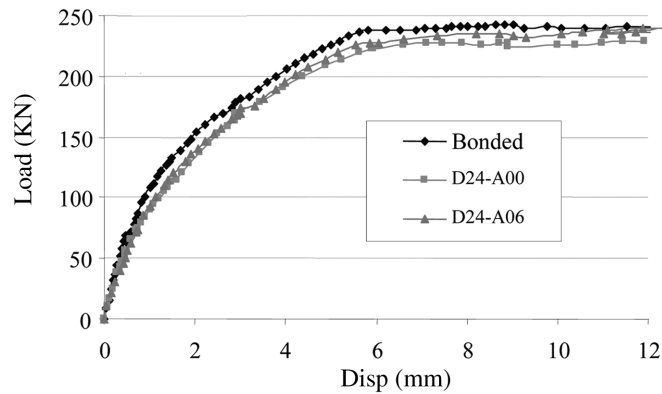


Fig. 6 Load-displacement curves for three designs (test)

to measure the axial displacements of both sides of the column, and then the rotation of the column and the horizontal displacement along the loading line are calculated.

The measured load-displacement curves for the lateral loading are shown in Fig. 6 for the three specimens, in which the load is the total lateral force executed on the column and the displacement is the lateral one at the middle point of the loading line (Point A). When the load is smaller than 60 KN, all the three designs are almost elastic; after that obvious non-linearity develops. When the displacement is 6 mm, all the designs start to yield. The loading forces that correspond to the yield points are 239 KN, 226 KN, and 224 KN respectively for the three designs. The experimental results show that the bonded design is a lit stronger and stiffer than the other two, and the un-bond design (D24-A00) is the weakest among the three.

The corresponding cracking patterns are shown in Fig. 7. Obviously the cracking in the first design is the worst among the three designs, i.e., it has more cracks in the column end than the other two. Hence, the introduction of the un-bonded zones effectively controls the cracking in the column end.

The details on the tests were reported in Teshigawara *et al.* (2004).
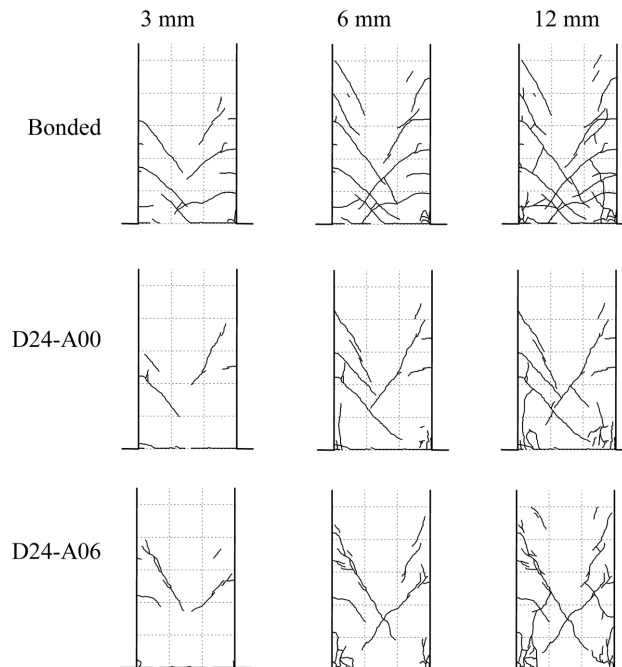
Fig. 7 Cracking patterns at displacements 3, 6, 12 mm

## 4. Finite element model for a column with a supporting base

Experimental tests are expensive and take long time; comparatively, a numerical method is economical and easy to be carried out. If its effectiveness and accuracy are verified by the experimental tests, a finite element model could be employed to conduct parametric studies of the influencing parameters and provide the most detailed information. It would serve as a design and evaluation tool.

In this analysis, a 2-dimensional model is employed. As main concerns are about cracking in column ends, hence a non-linear analysis is necessary to track the load-displacement process beyond the yielding of the column. A monotonous load is applied to the column at the height of 600 mm. In order to model the experimental loading condition (i.e., a strong clamp fixed along the loading line), all the points on the loading line (the height of 600 mm) are assumed to have the same horizontal displacement. The bottom edge of the base is fully constrained.

The finite element mesh (plane stress) is shown in Fig. 8. The element types and material properties are as follow.

**Concrete:** The concrete is modelled by 8-node iso-parametric elements. Only the corner nodes are shown in Fig. 8. The material properties of the concrete are: Young's modulus $E = 23900$ N/mm$^2$ and Poisson's ratio $v = 0.2$. The total strain crack model (DIANA 2002b), with an exponential relation for tension softening, is used. The tensile stress is assigned as $f_t' = 4.0$ N/mm$^2$ and the fracture energy $G_f = 0.15$ N·mm/mm$^2$ (Mechtcherime and Muller 2002). As no concrete crushing happens during the experiments, it is not necessary to consider compression softening in concrete.
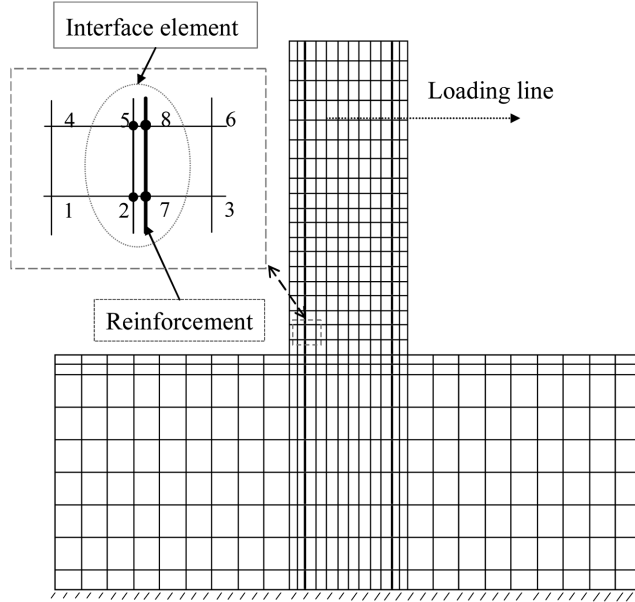
Fig. 8 Finite element mesh
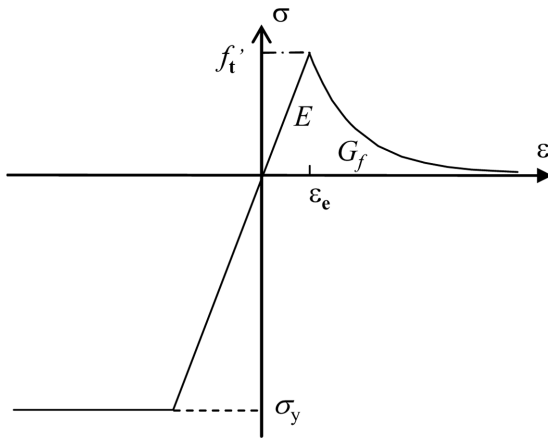


Fig. 9 Softening constitutive law of concrete
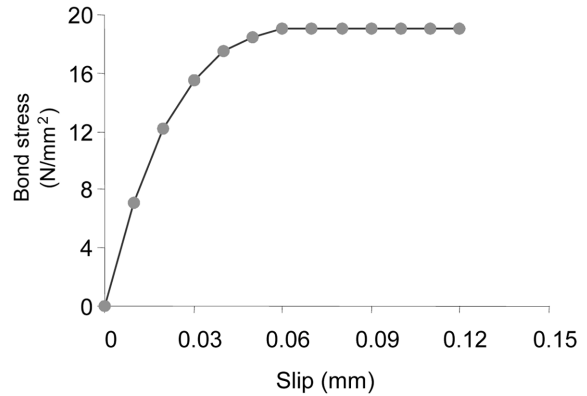


Fig. 10 Non-linear shear bond-slip relation

Therefore, concrete is simply assumed to be elastic-ideal-plastic for compression with a yield stress $\sigma_y = 23.5$ N/mm$^2$. The constitutive law of concrete is shown in Fig. 9.

**Bond:** The bond between concrete and reinforcing steel is modelled by interface elements (DIANA 2002a), as shown in Fig. 8. In Fig. 8, 1254 and 2365 are two concrete elements and 78 a steel element; nodes 7 and 8 are not connected to the concrete elements. The interfacial element is composed of nodes 2-7-5-8. The thickness of the interfacial elements is 0.1 mm. The normal bond slip is assumed to be linear and the stiffness is assigned as 1000 MPa/mm; the shear bond slip is assumed to be non-linear and follows Dorr model (as shown in Fig. 10)
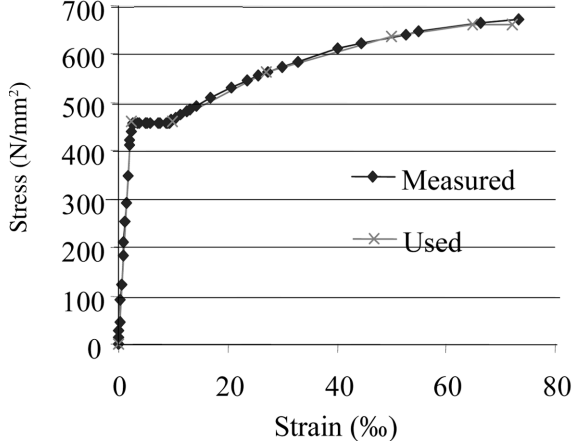
Fig. 11 Constitutive law of main re-bars
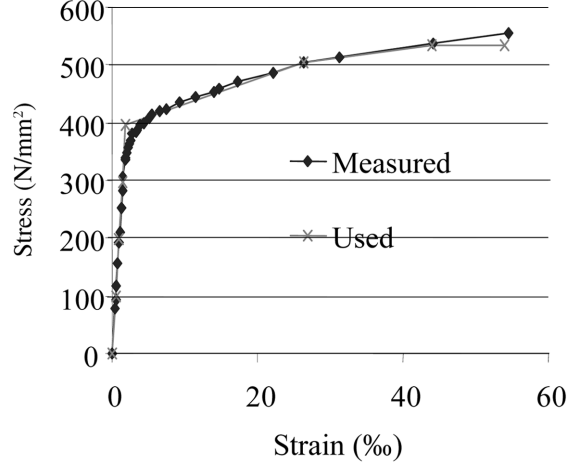
Fig. 12 Constitutive law of steel for additional and shear re-bars

$$
t_t = \begin{cases} f_t' \left[ 5\left(\dfrac{\Delta u_t}{\Delta u_t^0}\right) - 4.5\left(\dfrac{\Delta u_t}{\Delta u_t^0}\right)^2 + 1.4\left(\dfrac{\Delta u_t}{\Delta u_t^0}\right)^3 \right] & \text{if} \quad 0 \leq \Delta u_t < \Delta u_t^0 \\[4mm] 1.9 f_t' & \text{if} \quad \Delta u_t \geq \Delta u_t^0 \end{cases}
\tag{1}
$$

Where $\Delta u_t$ is the shear slip and $t_t$ the bond stress (shear); $f_t'$ is the tensile strength of the concrete and $\Delta u_t^0$ is the shear slip at which the curve becomes flat. The mechanical bond properties are strongly associated with the bar size of the reinforcing steel. The specific bond properties for the experimental tests are not available, therefore, $\Delta u_t^0 = 0.06$ mm is used as recommended by DIANA (2002a). The un-loading and re-loading stiffness for shear bond-slip is 250 MPa/mm (Popov 1984, Shima *et al.* 1987, Tassios and Yannopoulos 1981). The influences of the bond properties on cracking patterns in the column ends have been reported in authors' another paper (Chen *et al.* 2007). For un-bonded cases, both the normal and shear stiffness are simply assigned as 0.001 MPa/mm as the approximation of zero stiffness.

**Main reinforcing bars in column:** The main reinforcing bars are modelled by 3-node truss elements. Only the end nodes are shown in Fig. 8. The measured stress-strain curve is shown in Fig. 11; in the numerical analysis, a multi-linear relation is used to fit the measured curve. Young's modulus is $E = 210000$ N/mm$^2$, the initial yield stress $\sigma_y = 462$ N/mm$^2$, and the limit stress $\sigma_u = 661$ N/mm$^2$.

**Shear and additional reinforcing bars in column:** They are completely bonded with the surrounding concrete and therefore embedded in concrete elements (DIANA 2002a) in the numerical analysis. The measured stress-strain curve is shown in Fig. 12, with a initial yield stress, $\sigma_y = 382$ N/mm$^2$, and a limit stress, $\sigma_u = 534$ N/mm$^2$. Young's modulus is $E = 210000$ N/mm$^2$. A multi-linear relation is used to fit the measured curve in the numerical analysis.

**Solution procedure:** The loading set consists of a constant vertical force and a varying lateral displacement. First, the vertical force (425 KN) is applied and it is kept constant during the entire solution procedure. Secondly, a varying lateral displacement is applied incrementally. A Newton-Ralphson iteration scheme, with an energy-based convergence criterion, is employed to guarantee the convergence. As all the points on the loading line are assumed to have the same horizontal displacement, one point is defined as the master point and all the others slave points which have the same horizontal displacement as the master point. The reaction forces at all the points on the loading line are calculated and outputted as the reaction force which corresponds to the prescribed displacement.

## 5. Numerical analyses

### 5.1 Verification of finite element model

Fig. 13 shows the comparisons between the calculated and the measured load-displacement curves for the three designs. Generally speaking, the calculated results are fairly close to experimental ones. Obvious differences occur when the load is over 60 KN. Within the load range of [80, 180 KN], the calculated load-displacement curves are stiffer than the measured ones. Beyond this range, the calculated ones become flat quickly and have a similar strength as the experimental ones do. Yielding of the column occurs at 6 mm. The calculated yield strengths are 236 KN, 234 KN, and 235 KN respectively for the three designs and the experimental ones are 239 KN, 223 KN, and 226 KN. The differences between the calculated and experimental results may be caused by the uncertainty of the Young's modulus, tensile strength, fracture energy, and non-linear bond-slip. Inaccuracies also occur in measurements.

To verify the effectiveness of the finite element model, it is necessary to obtain the calculated cracking patterns and compare them with the experimental ones. Fig. 7 shows the measured cracking patterns caused by two-way loadings (both positive and negative directions of the cyclic loading). In experiments, the cracking for each direction is marked by a different color. For the purpose of comparison with the numerical results, the measured crack patterns for one-way loading are shown in Fig. 14.



|           (a) Bonded           |          (b) D24-A00           |          (c) D24-A06           |
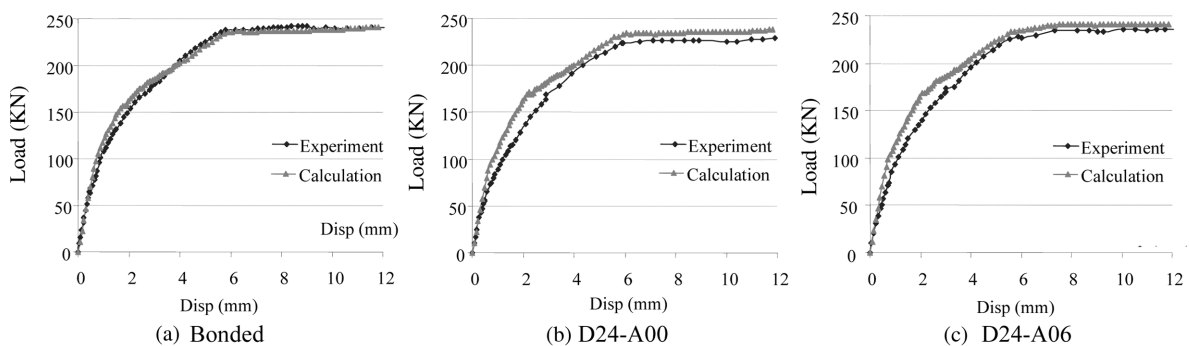
Fig. 13 Comparison of load-displacement curves between calculations and experiments
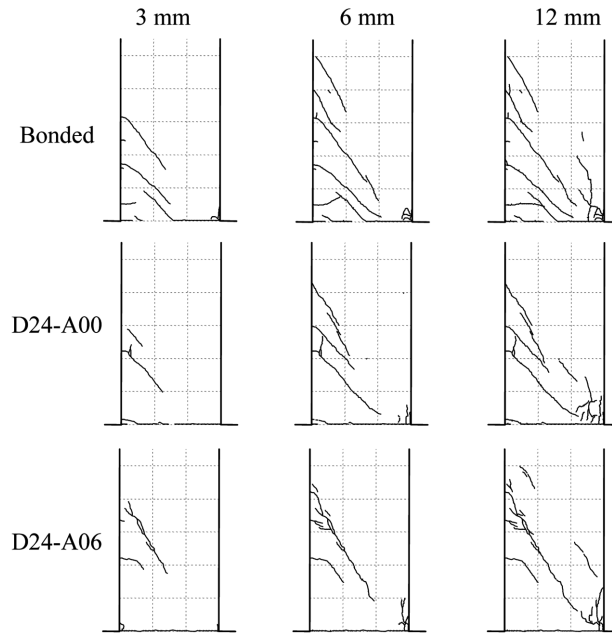
Fig. 14 Cracking patterns caused by one-way loading
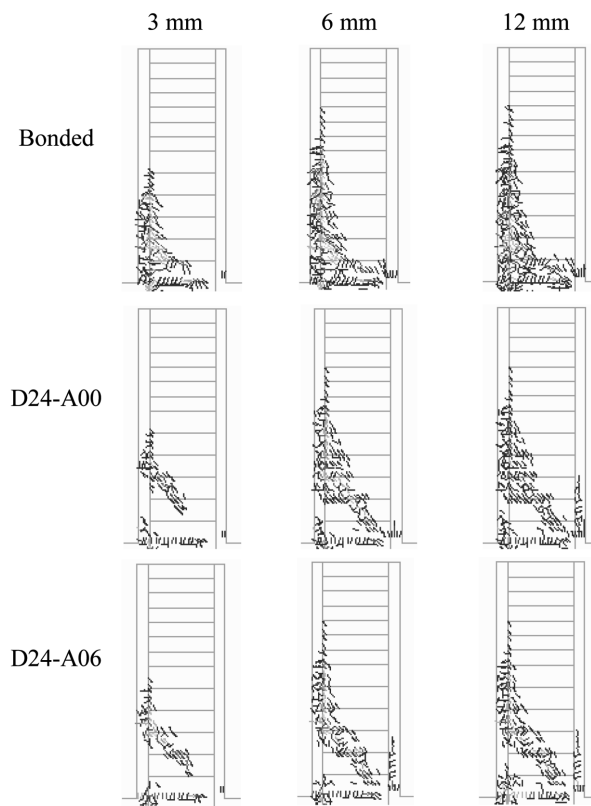
Fig. 15 Cracking patterns at 3, 6, and 12 mm (calculated)

The calculated cracking patterns for the three designs (bonded, D24-A00, and D24-A06) are shown in Fig. 15 at the prescribed displacements of 3 mm, 6 mm, and 12 mm. The calculating cracking patterns are comparable with the experimental ones, which are shown in Fig. 14. Obviously introducing un-bonded zones effectively controls cracking in the column end and adding additional re-bars slightly reduces cracking further.

## 5.2 The comparisons among the three designs

The main purpose is to find by finite element analysis a design which better controls cracking in column ends and has comparable stiffness and strength with those of the original bonded design.

The comparisons among the calculated load-displacement curves are shown in Fig. 16 for the three designs (bonded, D24-A00, and D24-A06). Unlike the measured results, the calculated load-displacement curves are very close to each other for the three designs. The calculated load-displacement curves demonstrate that the three designs have comparable stiffnesses and strengths. The bonded design is slightly stiffer than the other two, i.e., the introduction of un-bonded zones slightly reduces the stiffness as well as the limit strength of the column. Compared with the second one, the third design has a slight improvement in both the stiffness and the limit strength.

In Figs. 14 and 15, the cracking patterns are compared for the three designs at the same displacements, as the loading process is controlled by the prescribed displacement in the experiments and the cracking patterns are obtained against the displacement. In practice, no matter which design is used, the mass supported by the column will be the same. Hence, in earthquakes, the dynamic force acting on the column will be the same for each design. Therefore it is better to compare cracking patterns at the same load level.

The calculated cracking patterns for the three designs (bonded, D24-A00, and D24-A06) are shown in Fig. 17 at the load of 104 KN, 161 KN, 179 KN, 193 KN, and 217 KN.

At the load of 104 KN, all the three designs have similar cracking patterns in the critical section. The first design has the shortest crack and the second the longest one. For the first design, the cracking area develops upwards along the main re-bars in the tensile side; at the load of 161 KN, a diagonal shear crack starts to form. For the second and the third designs, as no force is transferred from the reinforcing bars to the concrete in the un-bonded zones, hence no cracking happens in
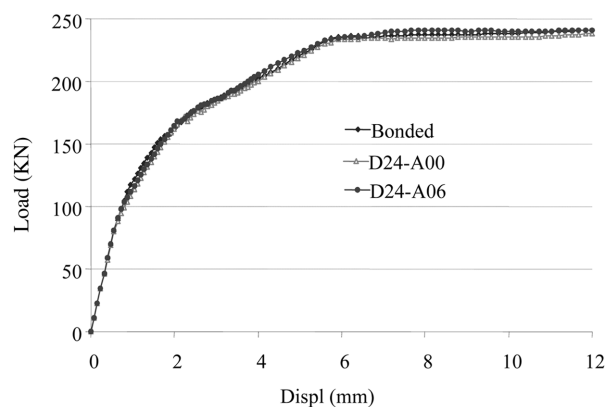


Fig. 16 Comparison of Load-displacement curves for three designs (Calculated)

Load=104 KN  Load=161 KN  Load=179 KN  Load=193 KN  Load=217KN

Bonded

D24-A00

D24-A06
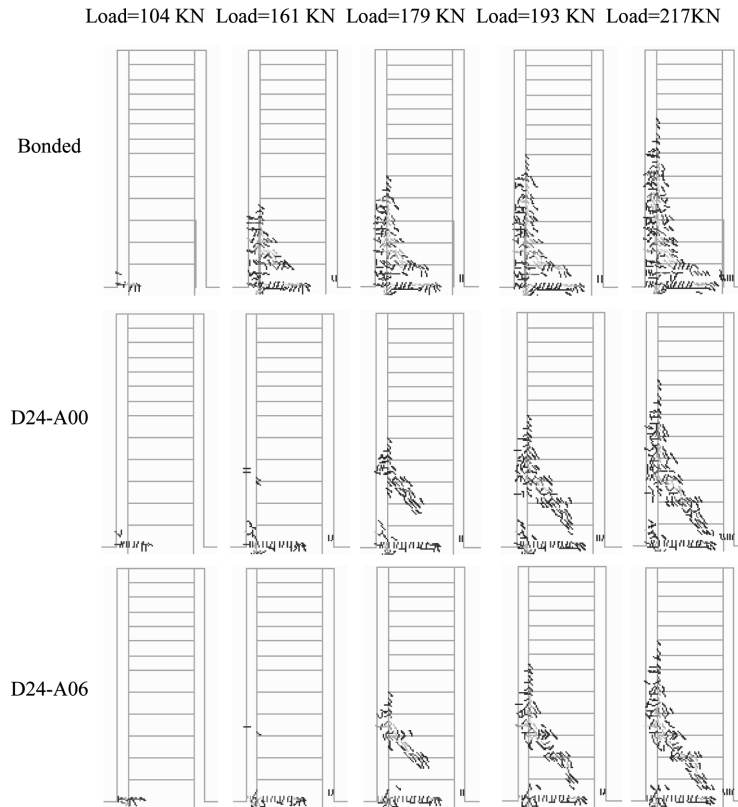
Fig. 17 Cracking patterns at loads 104 KN, 161 KN, 179 KN, 193 KN, and 217 KN

these areas; at the load of 161 KN, only very small cracks occur above the un-bonded zones. As this load is about 70% of the yield limit of the column, hence it is fair to say that the un-bonded designs effectively control the cracking in the column end.

At the load of 179 KN, for the first design the cracking area develops upwards further along the main re-bars in the tensile side; at the same time, a diagonal shear crack has formed. For the second and the third designs, a diagonal shear crack starts to form.

With the increase of the load, for the first design, the cracking pattern does not change thereafter and only the cracking strain increases. For the second and the third designs, a diagonal shear crack has formed at the load of 193 KN and the cracking pattern preserves thereafter.

In a word, among the three designs, the cracking in the first design is the worst and a shear crack forms first. Introducing the un-bonded zones effectively controls the cracking in the column; adding the additional reinforcing bars reduces cracking further.

## 6. Influences of un-bonded zones and additional reinforcement

Figs. 6 and 16 show that, the introduction of the un-bonded zones slightly reduces the stiffness and yield strength and adding additional reinforcing bars in the un-bonded zones improves stiffness
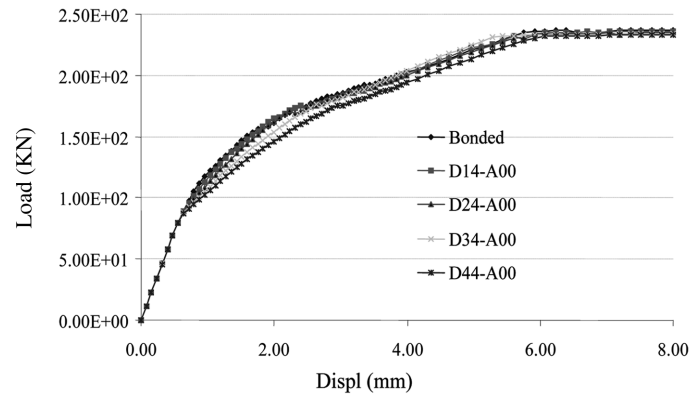
Fig. 18 Load-displacement curves for different lengths of un-bonded zones (Cal)

and yield strength somewhat. Therefore, in designing the un-bonded columns, it is significant to determine the length of the un-bonded zones and the amount of additional reinforcement to make the un-bonded columns best control cracking and have the equivalent stiffness and strength to those of the corresponding bonded column.

### 6.1 Influences of un-bonded zones

To investigate the influence of the un-bonded zone, a parametric study via finite element analysis has been carried out. Four cases with different lengths of un-bonded zones: 75 mm, 150 mm, 225 mm, and 300 mm (i.e., $\frac{1}{4}D$, $\frac{2}{4}D$, $\frac{3}{4}D$, and $\frac{4}{4}D$) are analyzed. Apart from the lengths of un-bonded zones, the other parameters are kept the same as in the bonded design. No additional reinforcement is added into the un-bonded zones. Fig. 18 plots the load–displacement curves obtained for the four cases by the finite element analyses. The results are compared with that of the bonded design.

Fig. 18 demonstrates that all the designs have almost the same strength and same linear part in the load-displacement curves. D14-A00 and D24-A00 have load–displacement curves that are very close to that of the bonded design; the load-displacement curve of D34-A00 has obvious difference from that of the bonded design within the load range [80, 200 KN] and the load–displacement curve of D44-A00 has a clear difference from those of the other designs. Generally speaking, the stiffness decreases with the increase of the length of the un-bonded zone, as the un-bonded zone prevents stress transfer from main re-bars to concrete, which leads to decreases in flexural and shear resistances.

The cracking patterns for the four cases are shown in Fig. 19 with the comparison with that of the bonded design. Obviously, the longer the length of the un-bonded zone is; the fewer cracks the column end has. In D34-A00, cracking is fairly prevented; and in D44-A00, cracking is totally prevented.

### 6.2 Influences of additional reinforcement

Fig. 19 shows that both D34-A00 and D44-A00 control cracking very well, and Fig. 18 indicates that D34-A00 is closer to the bonded design than D44-A00 in stiffness and strength. Hence among the four un-bonded designs, D34-A00 is the best one, which controls cracking better than D14-A00

Load=104 KN  Load=161 KN  Load=179 KN  Load=193 KN  Load=217KN

Bonded

D14-A00

D24-A00
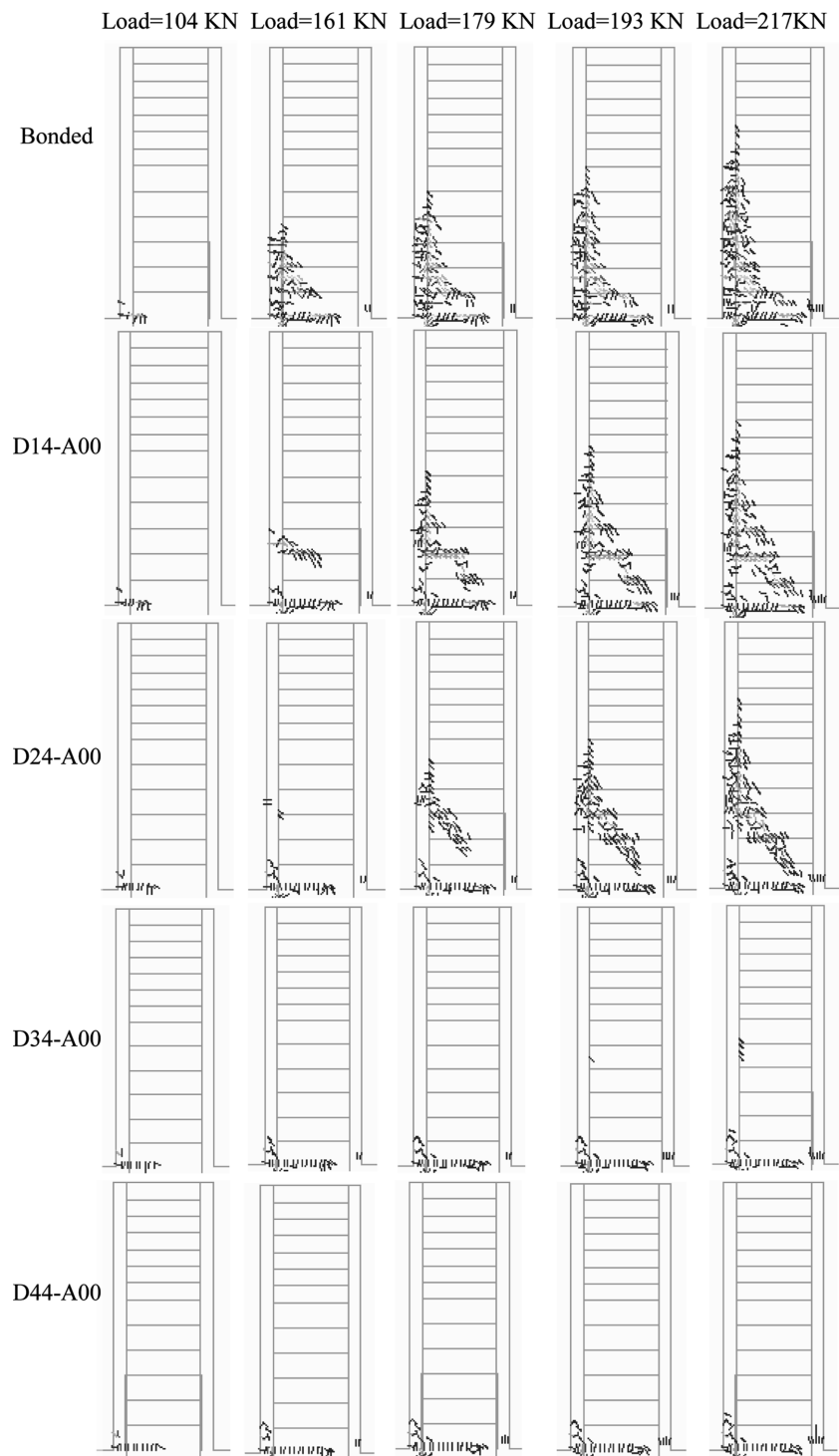
D34-A00

D44-A00

Fig. 19 Cracking patterns for different un-bonded zones at loads 104 KN, 161 KN, 179 KN, 193 KN, and 217 KN
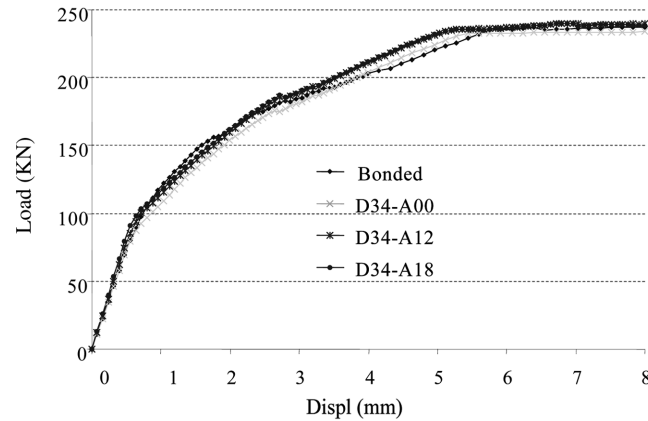
Fig. 20 Load-displacement curves for different sizes of additional re-bars

and D24-A00 and is stiffer than D44-A00.

As shown in Fig. 18, D34-A00 is clearly weaker than the bonded design in stiffness. It is expected that the stiffness can be enhanced through adding additional re-bars in the un-bonded zones. To determine the size of additional reinforcement, a parametric study via the finite element analysis is conducted. Two sizes (12 and 18 mm) of additional reinforcing bars are analyzed. Apart from the diameter of the additional reinforcement, the other parameters are kept the same as in D34-A00. It is assumed that the two sizes of additional reinforcing bars have the same material properties as shown in Fig. 12. Fig. 20 plots the load–displacement curves obtained for the two cases by the finite element analyses. The results are compared with those of the bonded design and D34-A00.

Fig. 20 shows that the stiffness and strength increase with the size of the additional reinforcement. Within the load range of [80, 160 KN], D34-A12 and D34-A18 have load-displacement curves very close to that of the bonded design. Beyond the load 160 KN, the load-displacement curves of D34-A12 and D34-A18 are stiffer than that of the original bonded design. Fig. 20 indicates that D34-A12 and D34-A18 are comparable with the original bonded design in stiffness and strength. Hence, additional reinforcing bars with a diameter between 12 and 18 mm are recommended.

## 7. Conclusions

This paper has developed a non-linear finite element model to study new column designs. The idea of introducing an un-bonded zone in the column end has been employed. The load-displacement curves and cracking patterns have been obtained and compared for these designs. The numerical results were verified by experimental results.

Through the experimental and numerical investigations, the following points should be highlighted

1. The numerical analyses were consistent with the experimental results and its effectiveness was verified by the experimental tests. Hence the finite element model established can serve as a design and evaluation tool and is able to provide detailed information via parametric studies
2. Both numerical and experimental studies indicated that the introduction of the un-bonded zone reduces cracking strain in the un-bonded zone (tensile side)

3. The proposed finite element model can be employed to decide the length of the un-bonded zone and the size of the additional reinforcing bars via parametric studies.

## Acknowledgements

## References

Bonacci, J. and Pantazopoulou, S. (1993), "Parametric investigation of joint mechanics", *ACI Struct. J.*, **90**(1), 61-71.

Chen, G., Fukuyama, H., Teshigawara, M., Etoh, H. and Kusunoki, K. (2007), "Parametric investigations on columns with un-bonded reinforcing bars for damage control", *Adv. Struct. Eng.*, **10**(2), 171-181.

DIANA. (2002a), "User's Manual - Element Library", TNO Building and Construction Research, Delft.

DIANA. (2002b), "User's Manual - Material Library", TNO Building and Construction Research, Delft.

Goto, Y., Joh, O. and Shibata, T. (1987), "Influence of lateral reinforcement in beam and joints on the behavior of R/C interior beam-column sub-assemblage", *Proc. of Japan Concrete Institute*, **9**, 187-192 (In Japanese).

Hakuto, S., Park, R. and Tanaka, H. (2000), "Seismic load tests on interior and exterior beam-column joints with substandard reinforcing details", *ACI Struct. J.*, **97**(1), 11-25.

Hallgren, M. and Bjerke, M. (2002), "Non-linear finite element analyses of punching shear failure of column footings", *Cement Concrete Compos.*, **24**(6), 491-496.

Hamada, O., Kamimura, T. and Hayashi, S. (1978), "Experimental study of reinforced concrete beam-column joints", *Proc. of Annual Meeting of Architecture Institute of Japan*, 1673-1674 (In Japanese).

Harumi Yashiro, Yasuo Tanaka, Masayuki Nagano, and Younggon Ro (1990), "Study on shear failure mechanisms of reinforced concrete short columns", *Eng. Fract. Mech.*, **35**(1-3), 277-289.

Hiraishi, H., Takagi, H., Nishio, K. and Yosikazu, K. (2004), "Reinforced concrete members with reinforcing bars yielding in steel sleeves", *In: 13th World Conf. on Earthquake Engineering*, August 2-6, Vancouver, Canada.

Ichinose, T. (1991), "Interaction between bond at beam bars and shear reinforcement in RC interior joints", In: Design of Beam-Column Joints for Seismic Resistance, J.O. Jirsa, ed., ACI, Detroit, 379-399.

Kashiwazaki, T. and Noguchi, H. (1994), "Nonlinear finite element analysis on shear and bond or RC interior beam-column joints with ultra high-strength materials", *Transactions Japan Concrete Inst.*, **16**, 509-516.

Maekawa, K. and An, X. (2000), "Shear failure and ductility of RC columns after yielding of main reinforcement", *Eng. Fract. Mech.*, **65**(2-3), 335-368.

Matsuoka, T., Ohkubo, M., Yoshioka, T., Morita, K. and Hashimoto, A. (1999), "Energy dissipation mechanism controlled by bottom bar yielding at beam end", *Proc. of Annual Meeting of Architecture Institute of Japan*, 913-914 (In Japanese).

Mau, S.T. (1990), "Numerical simulation of the behavior of axially loaded reinforced concrete columns", *Comput. Struct.*, **35**(4), 361-368.

Mazzoni, S. and Moehle, J.P. (2001), "Seismic response of beam-column joints in double-deck reinforced concrete bridge frames", *ACI Struct. J.*, **98**(3), 259-269.

Mechtcherime, V. and Muller, H.S. (2002), "Fracture behaviour of high-performance concrete", In: Finite Elements in Civil Engineering Applications, H.M.A.N. and R.J.G., eds., Balkema, Tokyo, 35-43.

Megget, L.M. (1973), "Exterior reinforced concrete joints with and without intersecting beams under seismic loading", *Bulletin Int. Institute of Seismology Earthq. Eng.*, **11**, 115-167.

Pandey, G.R. and Mutsuyoshi, H. (2005), "Seismic performance of reinforced concrete piers with bond-controlled reinforcements", *ACI Struct. J.*, **102**(2), 295-304.

Popov, E.P. (1984), "Bond and anchorage of reinforcing bars under cyclic loading", *J. Am. Concrete Inst.*, **81**(4), 340-349.

Saadeghvaziri, M.A. (1997), "Nonlinear response and modelling of RC columns subjected to varying axial load", *Eng. Struct.*, **19**(6), 417-424.

Shima, H., Chou, L. and Okamura, H. (1987), "Micro and Macro models for bond in reinforced concrete", *J. Faculty Eng. Univ. Tokyo (B)*, **39**(2), 133-194.

Tajima, Y., Kitayama, K., Okuda, M. and Kishida, S. (2000), "Influences of beam and column bar bond on failure mechanism in reinforced concrete interior beam-column joints", *Transactions Japan Concrete Inst.*, **22**, 433-440.

Tassios, T.P. and Yannopoulos, P.J. (1981), "Analytical studies on reinforced concrete members under cyclic loading based on bond stress-slip relationships", *J. Am. Concrete Inst.*, **78**(3), 206-216.

Teshigawara, M., Fukuyama, H., Kusunoki, K. and Etoh, H. (2004), "Experimental study on a new flexural reinforced concrete members with damage control in the yield hinge", *In: 13th World Conf. on Earthquake Engineering*, August 2-6, Vancouver, Canada.